University of Reading

Stratospheric impacts on weather regimes following the 2018 and 2019 sudden stratospheric Warmings

Article

Published Version

Creative Commons: Attribution 4.0 (CC-BY)

Open Access

Lee, R. W. ORCID: https://orcid.org/0000-0002-1946-5559, Charlton-Perez, A. J. ORCID: https://orcid.org/0000-0001-8179-6220 and Lee, S. H. (2025) Stratospheric impacts on weather regimes following the 2018 and 2019 sudden stratospheric Warmings. Geophysical Research Letters, 52 (15). e2025GL115668. ISSN 0094-8276 doi: 10.1029/2025GL115668 Available at https://centaur.reading.ac.uk/123726/

It is advisable to refer to the publisher's version if you intend to cite from the work. See Guidance on citing.

To link to this article DOI: http://dx.doi.org/10.1029/2025GL115668

Publisher: American Geophysical Union

All outputs in CentAUR are protected by Intellectual Property Rights law, including copyright law. Copyright and IPR is retained by the creators or other copyright holders. Terms and conditions for use of this material are defined in the End User Agreement.

University of Reading

www.reading.ac.uk/centaur

CentAUR

Central Archive at the University of Reading

Reading's research outputs online

Check for updates

AGU ADVANCING EARTH AND SPACE SCIENCES

Geophysical Research Letters

RESEARCH LETTER
10.1029/2025GL115668

Stratospheric Impacts on Weather Regimes Following the 2018 and 2019 Sudden Stratospheric Warmings

Robert W. Lee[1], **Andrew J. Charlton-Perez**[1], **and Simon H. Lee**[2]

[1]Department of Meteorology, University of Reading, Reading, UK, [2]School of Earth and Environmental Sciences, University of St Andrews, St Andrews, UK

Key Points:

- Using a stratospheric nudging protocol with operational subseasonal systems, we assess weather impacts from sudden stratospheric warmings (SSWs)
- SSWs consistently shift the atmospheric state toward negative North Atlantic Oscillation-style patterns
- Observed ridge-style patterns in the 2019 event suggests other forcings may override stratospheric impacts in subseasonal forecasts

Supporting Information:

Supporting Information may be found in the online version of this article.

Correspondence to:

R. W. Lee,
r.w.lee@reading.ac.uk

Citation:

Lee, R. W., Charlton-Perez, A. J., & Lee, S. H. (2025). Stratospheric impacts on weather regimes following the 2018 and 2019 sudden stratospheric warmings. *Geophysical Research Letters*, *52*, e2025GL115668. https://doi.org/10.1029/2025GL115668

Received 5 MAR 2025
Accepted 24 JUL 2025

Author Contributions:

Conceptualization: Robert W. Lee, Andrew J. Charlton-Perez, Simon H. Lee
Data curation: Robert W. Lee
Formal analysis: Robert W. Lee
Funding acquisition: Andrew J. Charlton-Perez
Investigation: Robert W. Lee, Andrew J. Charlton-Perez
Methodology: Robert W. Lee, Andrew J. Charlton-Perez, Simon H. Lee
Project administration: Robert W. Lee, Andrew J. Charlton-Perez
Software: Robert W. Lee, Simon H. Lee
Supervision: Andrew J. Charlton-Perez
Visualization: Robert W. Lee
Writing – original draft: Robert W. Lee, Andrew J. Charlton-Perez

© 2025. The Author(s).
This is an open access article under the terms of the Creative Commons Attribution License, which permits use, distribution and reproduction in any medium, provided the original work is properly cited.

Abstract Major disruptions of the stratospheric polar vortex can improve subseasonal forecast skill for surface climate, as negative North Atlantic Oscillation-like (NAO−) states can follow sudden stratospheric warmings (SSWs). Yet most insights come from observational studies or large operational forecast archives. Here we use Stratospheric Nudging And Predictable Surface Impacts (SNAPSI) project experiments, which applies stratospheric nudging to forecasts of two SSWs (2018 and 2019) followed by differing tropospheric evolutions. We show that SSWs systematically shift the atmosphere toward negative NAO-like regimes (stronger Greenland anticyclone) in both the North Atlantic-European and North American regions. Comparisons among *nudged*, *free*, and *control* runs quantify the benefits of improving and removing SSW representation in diagnosing tropospheric regime shifts. In 2018, accurate stratospheric representation improved weather regime forecasts. However, in 2019, despite persistent observed ridged regimes, *nudged* SSWs still induced negative NAO-like patterns, implying that subseasonal models sometimes underrepresent other teleconnections and overrepresent stratosphere-troposphere coupling.

Plain Language Summary Disruptions to the flow in the upper atmosphere, known as sudden stratospheric warmings (SSWs), can influence surface weather patterns weeks later (known as the subseasonal scale). These events can lead to weather patterns associated with unusually high pressure near Greenland, which can lead to unusually wintry weather over Europe and North America. However, most of the research that links SSWs and Greenland high has been based on observations or large model data sets rather than controlled experiments. In our study, we use targeted experiments from the Stratospheric Nudging And Predictable Surface Impacts project. These experiments adjust the upper atmospheric flow during two major warming events in 2018 and 2019 to better match observations. We examine how these changes affect weather patterns in the North Atlantic-European and North American regions. We show that by making the upper-atmosphere forecasts closely reproduce the SSWs, model forecasts are pushed toward predictions of a pattern involving high pressure over Greenland. Yet, in one event, the observed weather was characterized by wavy, ridge-like patterns instead. These case studies suggests that models sometimes do not fully capture other important influences and rely too much on the stratospheric link, limiting their subseasonal weather forecast skill.

1. Introduction

Variability in the stratosphere is often coupled with low-frequency tropospheric variability on subseasonal-to-seasonal (S2S) timescales during winter (e.g., Baldwin et al., 2003; Scaife et al., 2015; Sigmond et al., 2013; Tripathi et al., 2015). Anomalous stratospheric polar vortex (SPV) conditions, including sudden stratospheric warmings (SSWs), typically induce lower stratospheric conditions lasting several weeks to 2 months (Baldwin et al., 2024; Charlton & Polvani, 2007; Limpasuvan et al., 2004, 2005). On such timescales, large-scale tropospheric conditions represent "windows of opportunity" for skillful forecasts (Mariotti et al., 2020; Robertson et al., 2020). Weather regimes–recurrent, persistent, and quasi-stationary patterns (e.g., Michelangeli et al., 1995)–provide an ideal framework to identify these conditions and to diagnose how stratospheric anomalies can be viewed as a driver modulating weather regime transitions and persistence.

In the North Atlantic-European (NAE) sector winter regimes are NAO+, Atlantic Ridge, Scandinavian Blocking, NAO−; in the North American sector they are Pacific Trough, Arctic Low, Alaskan Ridge, and Arctic High (Figure S1 in Supporting Information S1). While defined by their mid-tropospheric flow patterns, their strong surface impacts make them useful to describe regional weather impacts on S2S timescales (Figure S2; Text S1 in

Writing – review & editing: Robert W. Lee, Andrew J. Charlton-Perez, Simon H. Lee

Supporting Information S1), supporting important forecast applications (e.g., Huang et al., 2020; van der Wiel et al., 2019; White et al., 2022).

In the NAE sector, the SPV most strongly modulates the NAO-like, zonally-oriented weather regimes (Beerli & Grams, 2019; Charlton-Perez et al., 2018; Domeisen et al., 2020), and the corresponding southern eddy-driven jet regime (Maycock et al., 2020). The regime present at SSW onset has been linked to post-SSW coupling (Domeisen et al., 2020).

In the North American sector, where the weather regimes cover a wider domain and incorporate both Atlantic and Pacific variability, three of the four regimes vary with SPV strength (these three regimes all feature low-wavenumber patterns) while the Alaskan Ridge does not (S. H. Lee et al., 2019, 2022). Nevertheless, downward wave reflection by the SPV can still trigger Alaskan Ridge transitions (Messori et al., 2022; Millin et al., 2022; Schutte et al., 2025). The Arctic High closely mirrors NAO− (Messori and Dorrington, 2023) and is associated with stratospheric planetary wave absorption (S. H. Lee et al., 2019; similar to cluster five in Kretschmer, Cohen, et al., 2018, Kretschmer, Coumou, et al., 2018).

While studies have demonstrated the stratospheric impact on weather regimes, much of our understanding stems from observational analyses or large forecast model archives. Knight et al. (2021) offered a distinct approach, employing targeted experiments to investigate influences surrounding two key case studies: the 2018 and 2019 boreal SSWs. Their full-field nudging approach separated tropical and stratospheric contributions, and removed initial condition sensitivity. They revealed that stratospheric forcing drove similar negative NAO-like (easterly) anomalies over Europe in both events. In contrast, tropical forcing led to opposing tropospheric responses: supporting NAO− in 2018 but promoting an Atlantic Ridge-like pattern with westerlies over Europe in 2019. Building on this, and focusing on the stratospheric component, the Stratospheric Nudging And Predictable Surface Impacts (SNAPSI; Hitchcock et al., 2022) protocol extends the analysis to a large set of the latest S2S forecast models. This enhanced multi-model experimental framework allows for a robust quantification of the direct SSW impact on weather regimes in these two case studies.

SNAPSI ran three main experiments: *free*, *control* and *nudged*. The *free* experiment represents a standard operational forecast where the atmosphere evolves freely after initialization. In the *control* experiment, the zonally symmetric stratospheric state is nudged toward a time-evolving climatological state. Whereas the *nudged* experiment nudges the zonally symmetric stratospheric state to the observed time-evolving state of the SSW event. Both observed and climatological states are derived from the ERA5 reanalysis (Hersbach et al., 2020). For both *nudged* and *control*, zonal-mean zonal wind and temperature are nudged above 90 hPa, ramping to full strength (6 hr timescale) by 50 hPa via a cubic profile, applied equally at all latitudes. The *control* setup gradually introduces its climatological reference state over the first 5 days to mitigate initialization shock. Each SSW event has two specified start dates: one several weeks prior, when the SSW is typically not well predicted in operational forecasts (and thus in *free*), and another closer to the event, when the SSW signal is present in the initial conditions (and thus at least partly represented in *free*). A small subset of models also ran two additional experiments: *control-full* and *nudged-full*, nudging the full (including zonally asymmetric) stratosphere; these are briefly discussed when relevant. Participating S2S models (Table S1 in Supporting Information S1) ran at least 50 members for integrations of at least 45 days.

In this study, to quantify SSW-driven changes, we calculate weather regimes in each ensemble. Comparing *nudged* and *free* simulations reveals how weather regimes would differ with an improved stratospheric forecast (based on imposed zonally symmetric stratospheric evolution). By contrast, comparing *nudged* and *control* simulations isolates the influence of the anomalous zonal-mean stratospheric evolution during SSWs on weather regime responses, noting that stratospheric asymmetries remain unconstrained in both experiments.

2. Calculating Weather Regimes

To quantify changes in winter weather regimes, we calculate observed and modeled regimes using an established clustering approach. This follows the combined methods of Cassou (2008), S. H. Lee et al. (2019), and R. W. Lee et al. (2019), starting with reanalysis data. We use 00Z data from the ERA5 reanalysis (Hersbach et al., 2020) for all November–March (NDJFM) days in the period 1 January 1979–31 March 2024 (a total of 6,886 days; leap days removed). Data are regridded to the common 1° SNAPSI grid. Geopotential height anomalies are calculated from daily 500 hPa fields by removing the seasonal cycle and linearly detrending with respect to the daily

19448007, 2025, 15, Downloaded from https://agupubs.onlinelibrary.wiley.com/doi/10.1029/2025GL115668 by Test, Wiley Online Library on [07/08/2025]. See the Terms and Conditions (https://onlinelibrary.wiley.com/terms-and-conditions) on Wiley Online Library for rules of use; OA articles are governed by the applicable Creative Commons License

10.1029/2025GL115668

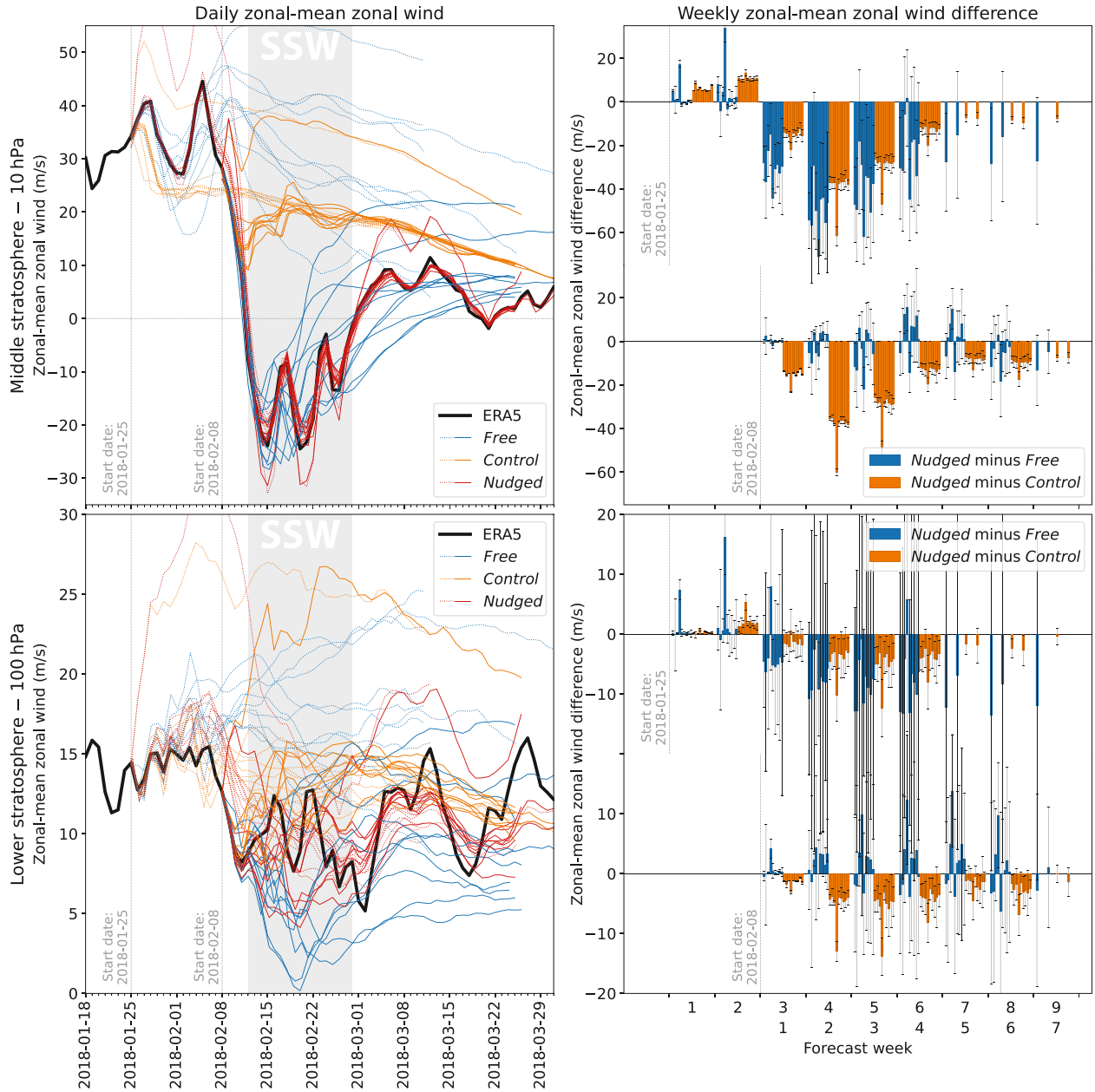

Figure 1. 2018 SSW: Zonal-mean zonal wind (left) and weekly *nudged* difference (right) at 60°N, 10 hPa (upper) and 100 hPa (lower). Gray shading indicated observed sudden stratospheric warming designation (negative zonal-mean zonal wind at 60°N, 10 hPa; Charlton & Polvani, 2007). Right panels' colored bars represent individual models sequentially (order: Table S1 in Supporting Information S1); error bars show twice the ensemble standard error. Vertical gray dashed lines (all panels) denote the two initialization start dates; right panel data for these dates are separated vertically and correspondingly shown on different *x*-axis levels. Left panel lines are dotted for the first and solid for the second start date.

climatology. Dimensionality is then reduced by applying an empirical orthogonal function (EOF; Hannachi et al., 2007) decomposition to square-root cosine latitude-weighted anomalies. This procedure is applied separately to the 90°W–30°E, 20–80°N sector (NAE regimes) and the 180–30°W, 20–80°N sector (North American regimes; Figure S1 in Supporting Information S1), retaining the leading 12 modes of variability. *k*-means clustering ($k = 4$) is performed using scikit-learn (Pedregosa et al., 2011). Each day is then assigned to a regime based on its minimum Euclidean distance to the cluster centroids. Data are then grouped by week to yield the fraction of each week in each regime, with the week's start day aligned to the first forecast start date for each SSW event. Weather regimes derived from this classification are shown in Figure S1 in Supporting Information S1.

19448007, 2025, 15, Downloaded from https://agupubs.onlinelibrary.wiley.com/doi/10.1029/2025GL115668 by Test, Wiley Online Library on [07/08/2025]. See the Terms and Conditions (https://onlinelibrary.wiley.com/terms-and-conditions) on Wiley Online Library for rules of use; OA articles are governed by the applicable Creative Commons License

10.1029/2025GL115668

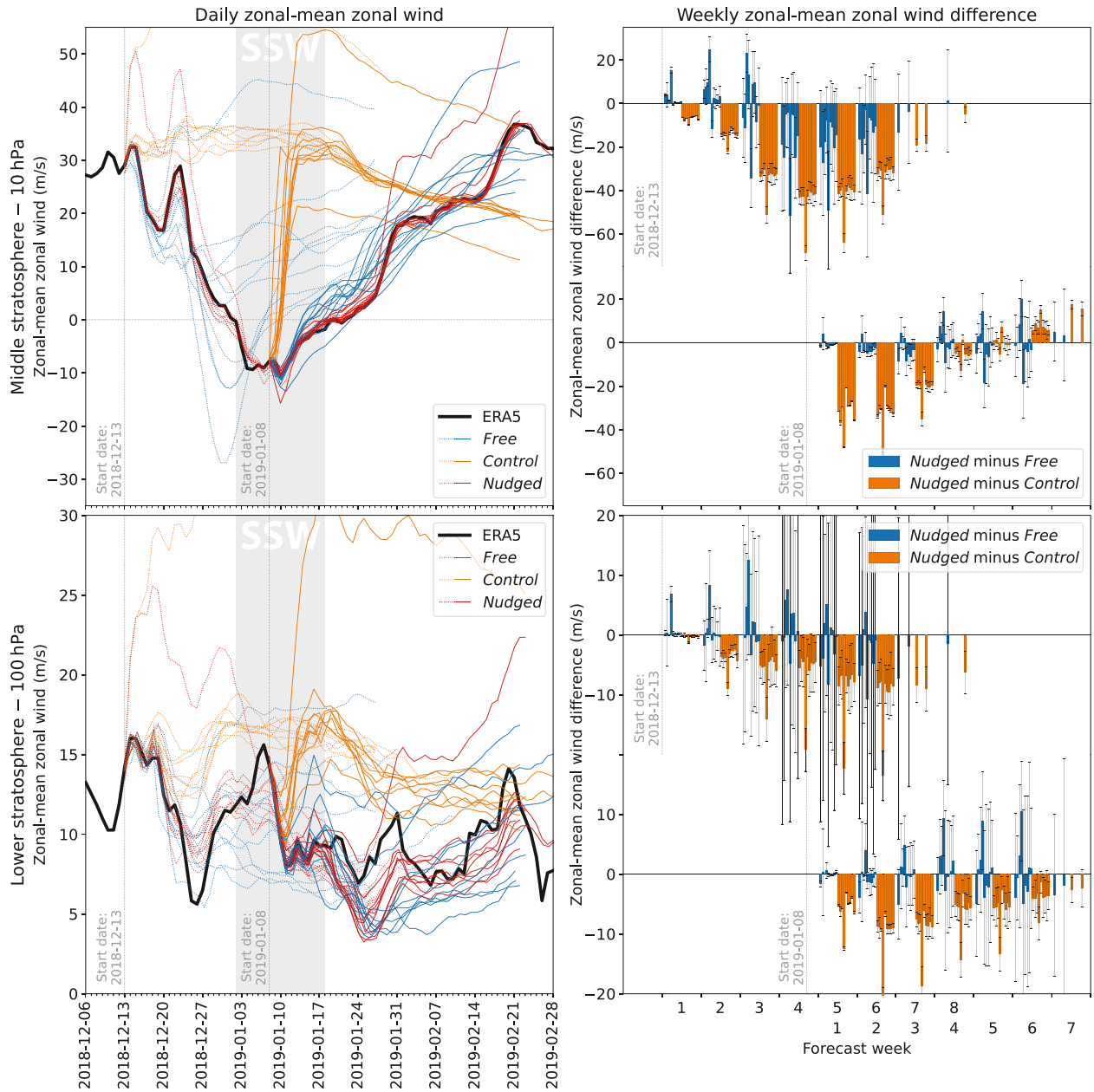

Figure 2. As Figure 1, but for the 2019 sudden stratospheric warming. Zonal-mean zonal wind (left) and weekly *nudged* difference (right) at 60°N, 10 hPa (upper) and 100 hPa (lower). Gray shading indicated observed sudden stratospheric warming designation (negative zonal-mean zonal wind at 60°N, 10 hPa; Charlton & Polvani, 2007). Right panels' colored bars represent individual models sequentially (order: Table S1 in Supporting Information S1); error bars show twice the ensemble standard error. Vertical gray dashed lines (all panels) denote the two initialization start dates; right panel data for these dates are separated vertically and correspondingly shown on different *x*-axis levels. Left panel lines are dotted for the first and solid for the second start date.

Next, we calculate weather regimes for the SNAPSI S2S models (Table S1 in Supporting Information S1). We use 00Z (or closest available) data for each model ensemble forecast experiment combination and regrid all data to the common 1° SNAPSI grid. For each forecast day, 500-hPa geopotential height anomalies are calculated by linear detrending relative to the ERA5 daily climatology. Pseudo-principal components are then calculated by projecting the forecast anomalies onto the 12 EOFs obtained from ERA5. Daily weather regime assignment for the forecast data is based on the ERA5 centroids by assigning the leading 12 pseudo-principal components to the cluster centroid with the minimum distance. Data are then grouped by week, matching the ERA5 regimes, to yield the fraction of ensemble members per week in each regime. Data are presented relative to ERA5 for maximum spatial comparability between observations and S2S model output. This approach allows systematic model biases,

19448007, 2025, 15, Downloaded from https://agupubs.onlinelibrary.wiley.com/doi/10.1029/2025GL115668 by Test, Wiley Online Library on [07/08/2025]. See the Terms and Conditions (https://onlinelibrary.wiley.com/terms-and-conditions) on Wiley Online Library for rules of use; OA articles are governed by the applicable Creative Commons License

10.1029/2025GL115668

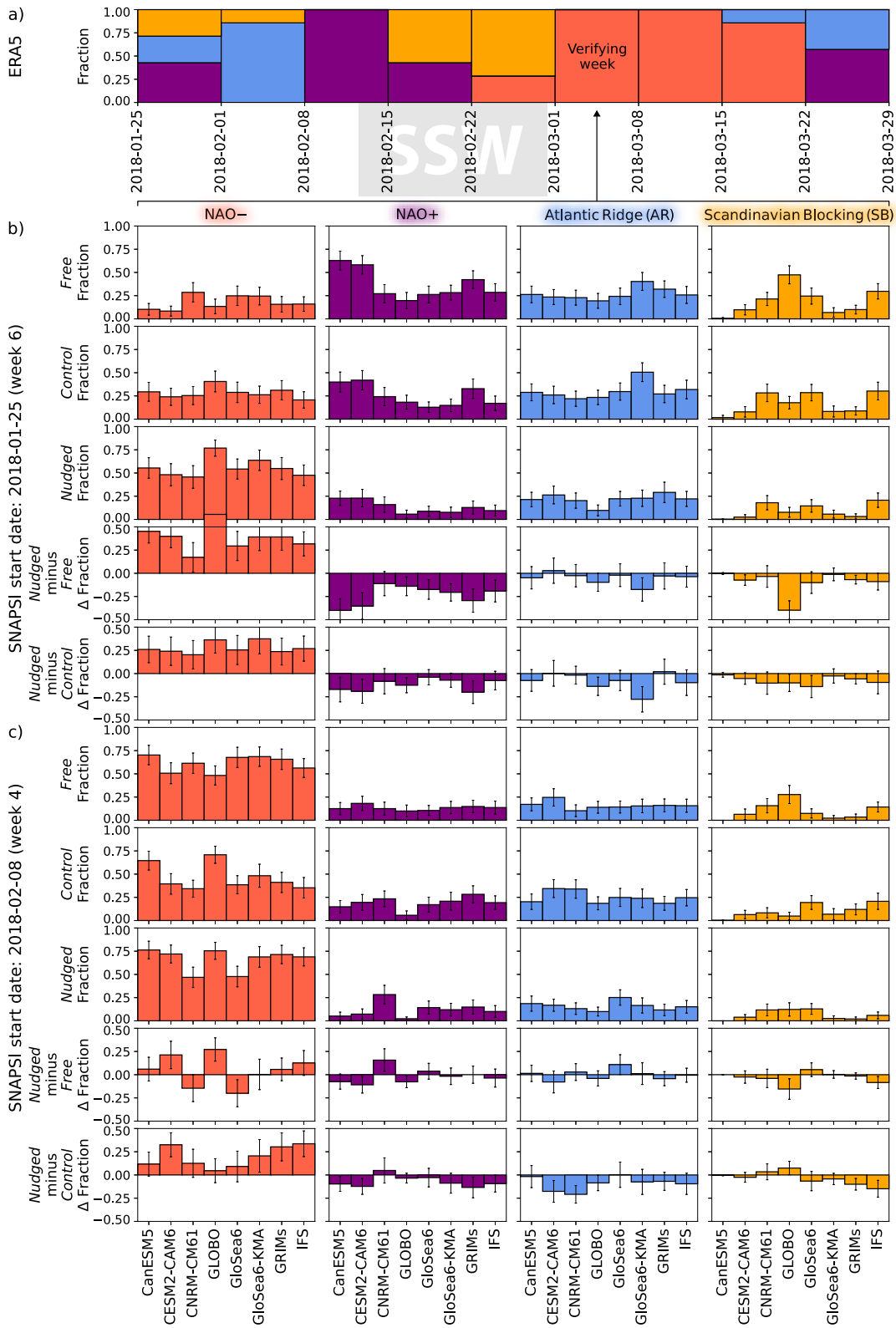

Figure 3.

19448007, 2025, 15, Downloaded from https://agupubs.onlinelibrary.wiley.com/doi/10.1029/2025GL115668 by Test, Wiley Online Library on [07/08/2025]. See the Terms and Conditions (https://onlinelibrary.wiley.com/terms-and-conditions) on Wiley Online Library for rules of use; OA articles are governed by the applicable Creative Commons License

19448007, 2025, 15, Downloaded from https://agupubs.onlinelibrary.wiley.com/doi/10.1029/2025GL115668 by Test, Wiley Online Library on [07/08/2025]. See the Terms and Conditions (https://onlinelibrary.wiley.com/terms-and-conditions) on Wiley Online Library for rules of use; OA articles are governed by the applicable Creative Commons License

such as differences in spatial pattern or anomaly amplitude, to be reflected in the regime classification, as in previous studies (e.g., van der Wiel et al., 2019). Projecting onto observed centers of action, this approach is analogous to other metrics (e.g., diagnosing SSWs via the zonal-mean zonal wind at 10 hPa, 60°N–Charlton, Polvani, Perlwitz, et al., 2007), and is the sole available option as corresponding hindcasts are not produced under SNAPSI protocols.

3. Sudden Stratospheric Warmings

Before examining the impact on the tropospheric weather regimes, we quantify stratospheric evolution differences between the sets of SNAPSI forecasts. We start with the SPV strength, calculated from the 10 hPa and 100 hPa zonal-mean zonal wind at 60°N (Charlton & Polvani, 2007), to identify the impact of the SNAPSI experimental protocols on SPV evolution as the SSWs evolve. As expected, the impact of the imposed nudging varies across the SSW lifecycle.

The left column of Figure 1 shows the evolution of zonal wind during the 2018 SSW, while the right column displays the weekly mean zonal wind difference, indicating the extent to which the nudging modifies the stratospheric state. As shown in the left column, the first set of *free* runs, initialized 2.5 weeks before the SSW onset, fail to predict the event (cf. Butler et al., 2020). The *control* runs damp the stratosphere toward a neutral, climatological state–resulting in a weaker polar vortex than the *free* runs for the first start date, and a stronger vortex than *free* for the second. *Nudging* forces the SSW at 10 hPa and also improves forecasts at 100 hPa, a key layer in coupling to large-scale tropospheric flow patterns below (Kautz et al., 2020). Full-field nudging experiments (not shown) fall well within the spread of the zonally symmetric experiments (at both levels, for both events). The strongest stratospheric disturbance (*nudged* minus *free* and *nudged* minus *control*; right column) occurs at week 4 (week commencing 2018-02-15) at 10 hPa and week 6 (w/c 2018-03-01) at 100 hPa (weeks relative to first start date), with *nudged* run differences being largest for the earlier start date. The slow, downward propagation of the SSW signal in the stratosphere is consistent with previous work (e.g., Baldwin et al., 2024).

For the first initialization of the 2019 SSW (Figure 2), while some *free* models predicted a major SSW and many others a minor warming, the zonal wind generally weakened and restored too early in the stratosphere. Compared to the 2018 event (Figure 1), most models exhibited much smaller differences between *nudged* and *free* simulations at 10 hPa, indicating improved free-running forecasts. The second start date, after SSW onset, saw nudging have a smaller impact at 10 hPa. At 100 hPa, nudging had modest corrective impacts; in some models, *nudged*-minus-*free* winds were positive, reflecting cases where the *free* runs predicted a warming that was too early and brief (leading to overly weak lower-stratospheric winds). Comparisons with the *control* runs again reveal the SSW's substantial influence throughout the stratosphere, with lower-stratospheric anomalies largest around week 6 (w/c 2019-01-17).

In one model (GEM-NEMO), the nudging appears to have been implemented incorrectly. At 10 hPa, the *nudged* zonal winds jump dramatically within the first day, while the *free* run exhibits similar jumps and a climatological profile much stronger than those of the other models. Given the consequent strengthening at 100 hPa, these errors appear to propagate downward throughout the atmosphere (see also the large differences evident in the longer bars in the right panels of Figures 1 and 2), and this model is therefore excluded from further analysis.

4. Weather Regime Response

Once the SSW perturbations reach the lower stratosphere, we observe a near-instantaneous tropospheric shift, consistent with literature (e.g., Baldwin & Dunkerton, 2001). Tropospheric impacts following an SSW can occur within a broad window up to 50 days after onset (Baldwin et al., 2024), varying between events. For the two events studied here, the strongest response in the lower stratosphere typically begins around 2 weeks after SSW

Figure 3. Observed and forecasted North Atlantic-European weather regimes associated with the 2018 sudden stratospheric warming (SSW). (a) ERA5 weather regime weekly fraction over the combined forecast period, from the first forecast start date to the end of the second. Gray shading denotes SSW designation. (b) Weekly fraction of ensemble members in a regime from forecasts for the week beginning 2018-03-01 ("verifying week"), originating from the first start date (2018-01-25; week 6 forecast). (c) As (b), but from the second start date (2018-02-08; week 4 forecast). Panels (b) and (c) display forecasts from the three Stratospheric Nudging And Predictable Surface Impacts experiments (*free*, *control*, *nudged*) and the difference between *nudged* and both *free* and *control* by S2S model. Forecast fraction uncertainty bars represent twice the ensemble standard error. All weekly fractions are aggregated from daily regime classifications.

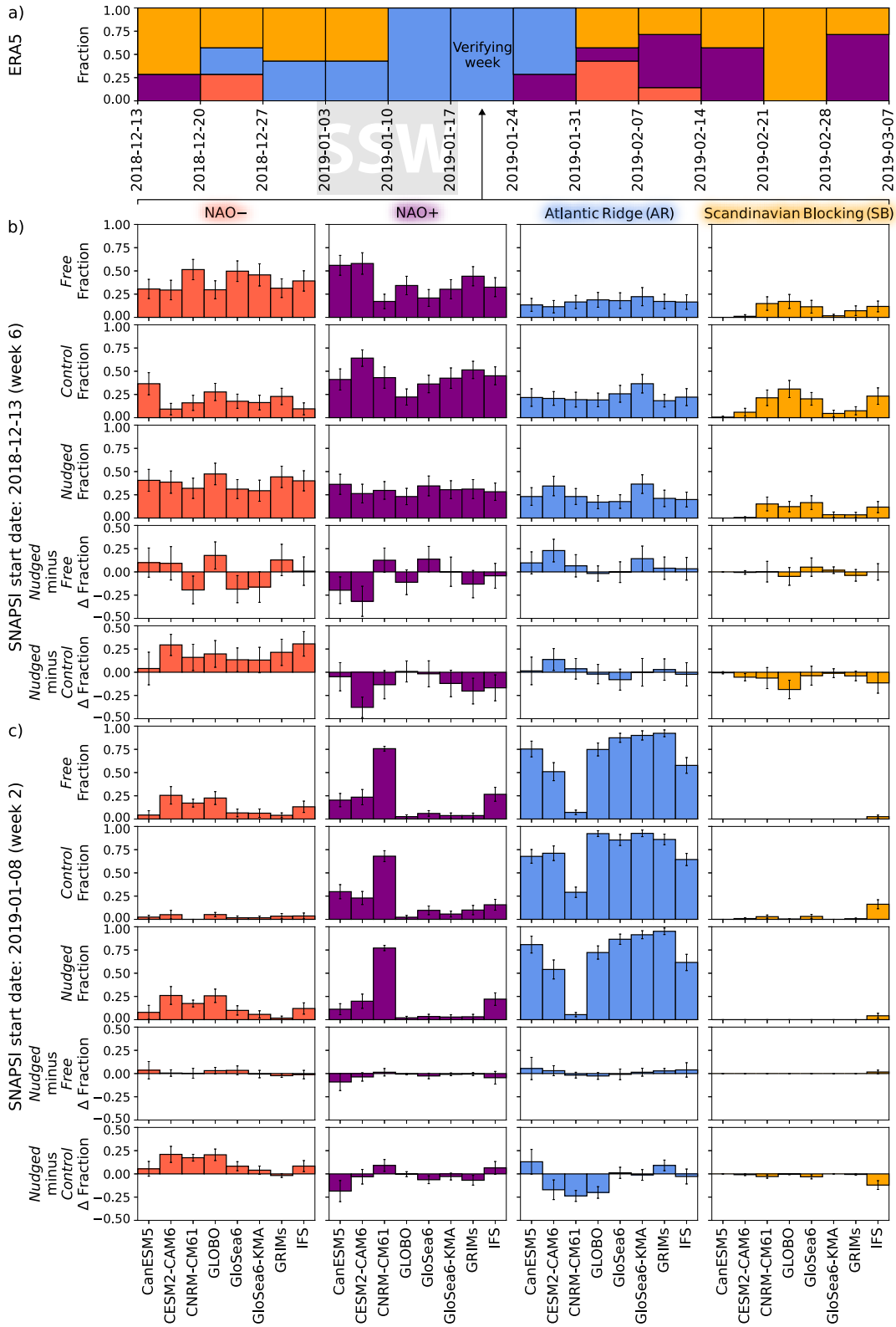

Figure 4.

19448007, 2025, 15, Downloaded from https://agupubs.onlinelibrary.wiley.com/doi/10.1029/2025GL115668 by Test, Wiley Online Library on [07/08/2025]. See the Terms and Conditions (https://onlinelibrary.wiley.com/terms-and-conditions) on Wiley Online Library for rules of use; OA articles are governed by the applicable Creative Commons License

19448007, 2025, 15, Downloaded from https://agupubs.onlinelibrary.wiley.com/doi/10.1029/2025GL115668 by Test, Wiley Online Library on [07/08/2025]. See the Terms and Conditions (https://onlinelibrary.wiley.com/terms-and-conditions) on Wiley Online Library for rules of use; OA articles are governed by the applicable Creative Commons License

onset (Section 3), corresponding to week 6 from the first initialization date. We therefore focus on this week, when tropospheric impacts are strongest, although the dominant regimes persist for longer.

For the 2018 event there are clear impacts on tropospheric weather regimes. In the NAE region, *nudged* runs show an NAO− regime response, consistent across models (Figure 3b). This doubles the proportion in the NAO− regime, making it the most likely regime, consistent with an expected stratospheric influence (with an even stronger shift to NAO− seen in the two models contributing to the *full-field nudging* of the SSW–Figure S3b in Supporting Information S1). This verifies well with the reanalysis, showing NAO− lasting over 2 weeks following the SSW (Figure 3a). *Free* runs generally do not produce forecasts with a dominant weather regime, though they show slightly larger fractions in the NAO+ and Atlantic Ridge regimes. *Control* runs exhibit a similar distribution, with an even more uniform split among regimes. The *nudged* differences from the *free* runs show an even greater shift to NAO− than relative to *control*. The shift toward NAO− in the *nudged* runs occurs at the expense of the other three regimes, with a relatively uniform reduction compared to the *control* runs, and a more pronounced reduction of NAO+ relative to the *free* runs, reflecting the continued strong polar vortex in those forecasts. By the second initialization (Figure 3c), NAO− becomes most likely in the *free* runs too, with the SSW being predicted.

For the 2019 SSW in the NAE region, following the first *free* runs, models are generally split between NAO− and NAO+ regimes (Figure 4b). *Control* runs tend to favor NAO+, while *nudged* runs slightly favor NAO− (and modestly more so under *full-field nudging*–Figure S4 in Supporting Information S1), similar to the impacts seen in the 2018 SSW. While *nudged* differences relative to *free* are mixed, partly due to some runs capturing early SSWs, differences relative to *control* highlight the role of the SSW in shifting regimes toward NAO− across models. However, unlike in 2018, reanalysis shows that the verifying regime following the SSW was Atlantic Ridge (Figure 4a). *Nudging* only slightly increases the likelihood of Atlantic Ridge (and slightly less so under *nudging-full*) which remains the third most likely regime, with NAO− being the most likely. This contrasts sharply with the 2018 event, where *nudging* doubled the probability of the verifying regime (NAO−). By the second initialization (Figure 4c), the SSW had already begun and with the shorter lead time (2 weeks), most models correctly predicted Atlantic Ridge, with negligible *nudged*-minus-*free* differences. *Nudged*-minus-*control* differences shift slightly toward NAO− at the expense of Atlantic Ridge, reflecting the impact of persisting the SSW, compared to the quick recovery seen in the *control*. CNRM-CM 6.1 shows unusually high NAO+ fractions across all runs from this start date, suggesting a possible state-dependent bias related to initial conditions and/or model formulation.

Similar patterns emerge when examining the impact of nudging on North American weather regimes during the 2018 and 2019 SSWs. In the 2018 event (Figure 5), *nudged* model runs show an increased likelihood of the verifying Arctic High regime (with an even stronger Arctic High response under *full nudging*–Figure S5 in Supporting Information S1), mirroring the NAO− shift seen in the NAE region. This proportion approximately doubles from *free* to *nudged* runs, elevating Arctic High from the least to the most likely regime at longer lead times (week 6), consistent with stratospheric nudging. By the second start date, with the SSW already forecasted in the *free* runs, *nudging* accordingly leads to smaller and more model-dependent changes.

For the 2019 SSW (Figure S6 in Supporting Information S1), forecasts in the North American region exhibit a broad spread across regimes, with model-dependent differences relative to the *free* runs. The *nudged*-minus-*control* results indicate a slight shift toward an Arctic High response following the SSW, similar to 2018 (and modestly more so under *nudged-full*–Figure S7 in Supporting Information S1). However, as in the NAE region, a key difference emerges: there is no substantial increase in the likelihood of the verifying Alaskan Ridge regime in the *nudged* runs, except in a few models at short lead times (2 weeks).

Figure 4. As Figure 3, but for the 2019 sudden stratospheric warming (SSW). Observed and forecasted North Atlantic-European weather regimes. (a) ERA5 weather regime weekly fraction over the combined forecast period, from the first forecast start date to the end of the second. Gray shading denotes SSW designation. (b) Weekly fraction of ensemble members in a regime from forecasts for the week beginning 2019-01-17 ("verifying week"), originating from the first start date (2018-12-13; week 6 forecast). (c) As (b), but from the second start date (2019-01-08; week 2 forecast). Panels (b) and (c) display forecasts from the three Stratospheric Nudging And Predictable Surface Impacts experiments (*free*, *control*, *nudged*) and the difference between *nudged* and both *free* and *control* by S2S model. Forecast fraction uncertainty bars represent twice the ensemble standard error. All weekly fractions are aggregated from daily regime classifications.

10.1029/2025GL115668

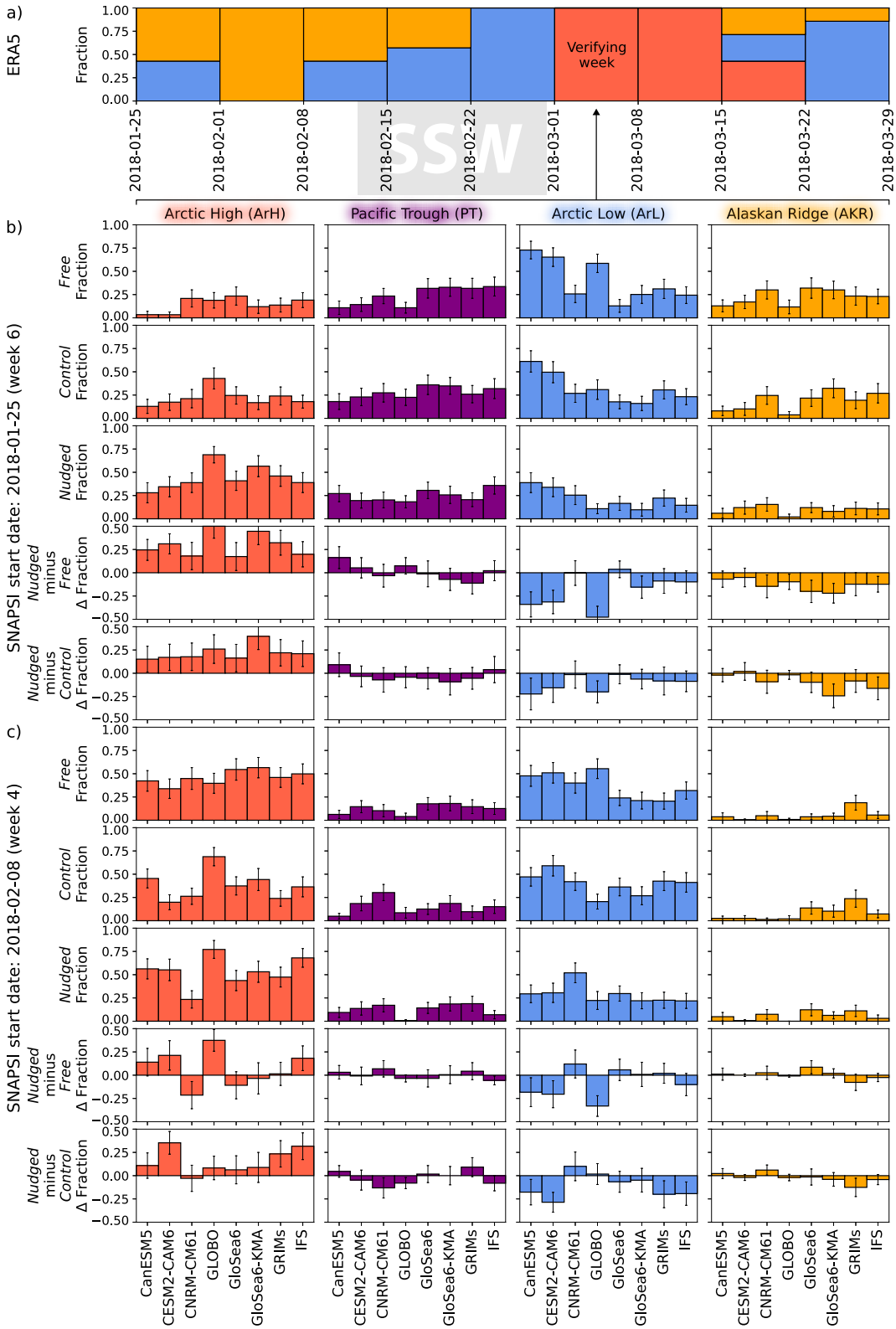

Figure 5.

19448007, 2025, 15, Downloaded from https://agupubs.onlinelibrary.wiley.com/doi/10.1029/2025GL115668 by Test, Wiley Online Library on [07/08/2025]. See the Terms and Conditions (https://onlinelibrary.wiley.com/terms-and-conditions) on Wiley Online Library for rules of use; OA articles are governed by the applicable Creative Commons License

19448007, 2025, 15, Downloaded from https://agupubs.onlinelibrary.wiley.com/doi/10.1029/2025GL115668 by Test, Wiley Online Library on [07/08/2025]. See the Terms and Conditions (https://onlinelibrary.wiley.com/terms-and-conditions) on Wiley Online Library for rules of use; OA articles are governed by the applicable Creative Commons License

5. Summary and Discussion

The SNAPSI experiments a enable robust, explicit assessment of the influence of the stratospheric state on tropospheric weather regimes for the first time. For the 2018 and 2019 SSWs examined in these nudging experiments, a common influence is clear across many models: SSWs push the tropospheric state toward regimes characterized by an anomalous Greenland anticyclone (NAO− and Arctic High). This is consistent with previous modeling studies, which found the imposed stratospheric signal leads to a generally linear shift in the troposphere (Kautz et al., 2020; Knight et al., 2021; White et al., 2020), though this does not always translate into improved regime forecast skill for individual events (S. H. Lee et al., 2022).

Following the onset of the 2018 event, there was a shift toward blocked regimes: NAO− in the NAE region and Arctic High (its analog) in the North American region. In forecasts where the stratosphere was nudged toward observations and initialized many weeks before the SSW (when it was poorly predicted), nudging doubled the frequency of these regimes, raising their rank from third or second among the four regimes. This suggests that a more accurate SSW forecast would have improved predictions of the dominant weather regime in each region. This response is even more pronounced when full-field (instead of zonally symmetric) stratospheric nudging is applied, which more tightly constrains planetary wave evolution. The results are also more pronounced when compared to *control* runs, where the SSW was removed.

For the 2019 event, nudging to the observed stratospheric state similarly increased the occurrence of NAO− and Arctic High within the forecasts, as in the 2018 event, particularly when compared to *control* runs. However, for this event, the verifying regimes were Atlantic Ridge (NAE region) and Alaskan Ridge (North American region). While nudging slightly increased the likelihood of Atlantic Ridge in some models, it remained only the third most likely regime.

This SNAPSI-based analysis of two SSW events shows that when the stratosphere is strongly perturbed, tropospheric responses match those identified in observational studies (e.g., Beerli & Grams, 2019; Charlton-Perez et al., 2018; Domeisen et al., 2020; S. H. Lee et al., 2019), confirming their stratospheric origin. While we only consider two events here, the findings provide confidence that the well-documented tropospheric response to an SSW is robust across models and applicable to a wide range of cases.

While the broad-scale influence of the 2018 and 2019 SSWs similarly pushed the atmosphere toward NAO-like states, the verifying regimes differed. The Atlantic Ridge and Alaskan Ridge regimes persisted for over 2 weeks, longer than climatology, indicating increased regime persistence. This strongly suggests the presence of additional forcing(s) in the system, such as the MJO. Supporting this, Knight et al. (2021) demonstrated that while stratospheric forcing drove similar easterly anomalies in both events, differences in tropical activity resulted in opposing impacts on the NAE sector.

The results also suggest that models overestimate stratosphere-to-troposphere coupling. This is consistent with Erner and Karpechko (2024), who found an increase in cold air outbreak false alarms during the decay of weak vortex events. It also aligns with Garfinkel et al. (2025), where at least half of assessed S2S models, as well as the multi-model mean, showed that the downward coupling was too strong. For the 2018 event, González-Alemán et al. (2021) showed that the troposphere became receptive to the SSW signal only after two cyclogenesis events, highlighting a stepwise increase in predictability resulting in the Greenland anticyclone (NAO−); without these developments, a predictability barrier remained.

The forecast "bust" across models for the 2019 SSW suggests improved stratospheric forecasts alone do not guarantee better tropospheric regime predictions. Running SNAPSI-style experiments across hindcast sets could enable assessments of statistical reliability, while tropical-nudging SNAPSI experiments would help determine whether any multi-model consensus exists in tropical forcing. Further research is needed to understand the

Figure 5. As Figure 3, but for the observed and forecasted North American weather regimes, associated with the 2018 sudden stratospheric warming (SSW). (a) ERA5 weather regime weekly fraction over the combined forecast period, from the first forecast start date to the end of the second. Gray shading denotes SSW designation. (b) Weekly fraction of ensemble members in a regime from forecasts for the week beginning 2018-03-01 ("verifying week"), originating from the first start date (2018-01-25; week 6 forecast). (c) As (b), but from the second start date (2018-02-08; week 4 forecast). Panels (b) and (c) display forecasts from the three Stratospheric Nudging And Predictable Surface Impacts experiments (*free*, *control*, *nudged*) and the difference between *nudged* and both *free* and *control* by S2S model. Forecast fraction uncertainty bars represent twice the ensemble standard error. All weekly fractions are aggregated from daily regime classifications.

19448007, 2025, 15, Downloaded from https://agupubs.onlinelibrary.wiley.com/doi/10.1029/2025GL115668 by Test, Wiley Online Library on [07/08/2025]. See the Terms and Conditions (https://onlinelibrary.wiley.com/terms-and-conditions) on Wiley Online Library for rules of use; OA articles are governed by the applicable Creative Commons License

dynamical role of additional forcings in weather regime transitions and persistence during these events. A storylines approach could be used to examine whether specific subsets of S2S models, ensemble members, and experiments (with and without active MJO events) featured teleconnections which contributed to the ridge-like regimes observed in 2019, overriding the stratospheric forcing. Additionally, further analysis could explore differing SSW characteristics in these experiments, particularly regarding wave-1 versus wave-2 and split versus displacement events (e.g., Kretschmer, Cohen, et al., 2018, Kretschmer, Coumou, et al., 2018).

Data Availability Statement

This work is based on SNASPI data, following the SNAPSI protocol (Hitchcock et al., 2022). The SNAPSI data are available from the Centre for Environmental Data Analysis (CEDA) archive, a UK-based repository, part of the Natural Environment Research Council's (NERC) Environmental Data Service (EDS). The models are available from the following CEDA sources: CanESM5 (Anstey et al., 2025), CESM2-CAM6 (Simpson & Richter, 2024), CNRM-CM 6.1 (Specq, 2024), GEM-NEMO (Lin & Muncaster, 2024), GLOBO (Mastrangelo, 2024), GloSea6 (Knight, 2024), GloSea6-KMA (GloSea6-GC3.2; Kim & Hyun, 2024), GRIMs (Son & Hong, 2024), IFS (Hitchcock et al., 2024), NAVGEM (Barton, 2025). ERA5 hourly data on pressure and surface levels used in the study was obtained from the Copernicus Climate Change Service (C3S) Climate Data Store (CDS) at Hersbach et al. (2023), Hersbach et al. (2023a, 2023b). EOF and k-means clustering analysis were performed using the freely available Python packages “eofs” (Dawson, 2016) and “scikit-learn” (Pedregosa et al., 2011), respectively.

Acknowledgments
RWL and AJCP were supported by the University of Reading. We thank the two anonymous reviewers for their constructive comments, which helped improve the clarity and robustness of this manuscript. This work used JASMIN, the UK's collaborative data analysis environment (https://www.jasmin.ac.uk).

References

Anstey, J., Kharin, V., & Sigmond, M. (2025). Stratospheric Nudging And Predictable Surface Impacts (SNAPSI): Data produced by the CanESM5 model at CCCma [Dataset]. *NERC EDS Centre for Environmental Data Analysis*. http://catalogue.ceda.ac.uk/uuid/01dac4c57559407fb40292389c386d30/

Baldwin, M. P., Birner, T., & Ayarzagüena, B. (2024). Tropospheric amplification of stratosphere–troposphere coupling. *Quarterly Journal of the Royal Meteorological Society*, *150*(765), 5188–5205. https://doi.org/10.1002/qj.4864

Baldwin, M. P., & Dunkerton, T. J. (2001). Stratospheric harbingers of anomalous weather regimes. *Science*, *294*(5542), 581–584. https://doi.org/10.1126/science.1063315

Baldwin, M. P., Stephenson, D. B., Thompson, D. W., Dunkerton, T. J., Charlton, A. J., & O'Neill, A. (2003). Stratospheric memory and skill of extended-range weather forecasts. *Science*, *301*(5633), 636–640. https://doi.org/10.1126/science.1087143

Barton, C. (2025). Stratospheric Nudging And Predictable Surface Impacts (SNAPSI): Data produced by the NAVGEM model at NRL [Dataset]. *NERC EDS Centre for Environmental Data Analysis*. http://catalogue.ceda.ac.uk/uuid/ecad5261e8d446bfa842b4b7a227d5b0/

Beerli, R., & Grams, C. M. (2019). Stratospheric modulation of the large-scale circulation in the Atlantic–European region and its implications for surface weather events. *Quarterly Journal of the Royal Meteorological Society*, *145*(725), 3732–3750. https://doi.org/10.1002/qj.3653

Butler, A. H., Lawrence, Z. D., Lee, S. H., Lillo, S. P., & Long, C. S. (2020). Differences between the 2018 and 2019 stratospheric polar vortex split events. *Quarterly Journal of the Royal Meteorological Society*, *146*(732), 3503–3521. https://doi.org/10.1002/qj.3858

Cassou, C. (2008). Intraseasonal interaction between the Madden–Julian oscillation and the North Atlantic oscillation. *Nature*, *455*(7212), 523–527. https://doi.org/10.1038/nature07286

Charlton, A. J., & Polvani, L. M. (2007). A new look at stratospheric sudden warmings. Part I: Climatology and modeling benchmarks. *Journal of Climate*, *20*(3), 449–469. https://doi.org/10.1175/JCLI3996.1

Charlton, A. J., Polvani, L. M., Perlwitz, J., Sassi, F., Manzini, E., Shibata, K., et al. (2007). A new look at stratospheric sudden warmings. Part II: Evaluation of numerical model simulations. *Journal of Climate*, *20*(3), 470–488. https://doi.org/10.1175/jcli3994.1

Charlton-Perez, A. J., Ferranti, L., & Lee, R. W. (2018). The influence of the stratospheric state on North Atlantic weather regimes. *Quarterly Journal of the Royal Meteorological Society*, *144*(713), 1140–1151. https://doi.org/10.1002/qj.3280

Dawson, A. (2016). eofs, A library for EOF analysis of meteorological, oceanographic, and climate data. *Journal of Open Research Software*, *4*(1), 14. https://doi.org/10.5334/jors.122

Domeisen, D. I. V., Grams, C. M., & Papritz, L. (2020). The role of North Atlantic–European weather regimes in the surface impact of sudden stratospheric warming events. *Weather and Climate Dynamics*, *1*(2), 373–388. https://doi.org/10.5194/wcd-1-373-2020

Erner, I., & Karpechko, A. (2024). Factors influencing subseasonal predictability of northern Eurasian cold spells. *Quarterly Journal of the Royal Meteorological Society*, *150*(762), 2955–2975. https://doi.org/10.1002/qj.4744

Garfinkel, C. I., Lawrence, Z. D., Butler, A. H., Dunn-Sigouin, E., Erner, I., Karpechko, A. Y., et al. (2025). A process-based evaluation of biases in extratropical stratosphere–troposphere coupling in subseasonal forecast systems. *Weather and Climate Dynamics*, *6*(1), 171–195. https://doi.org/10.5194/wcd-6-171-2025

González-Alemán, J. J., Grams, C. M., Ayarzagüena, B., Zurita-Gotor, P., Domeisen, D. I. V., Gómara, I., et al. (2021). Tropospheric role in the predictability of the surface impact of the 2018 sudden stratospheric warming event. *Geophysical Research Letters*, *49*, e2021GL095464. https://doi.org/10.1029/2021gl095464

Hannachi, A., Jolliffe, I. T., & Stephenson, D. B. (2007). Empirical orthogonal functions and related techniques in atmospheric science: A review. *International Journal of Climatology*, *27*(9), 1119–1152. https://doi.org/10.1002/joc.1499

Hersbach, H., Bell, B., Berrisford, P., Biavati, G., Horányi, A., Muñoz Sabater, J., et al. (2023a). ERA5 hourly data on pressure levels from 1940 to present [Dataset]. *Copernicus Climate Change Service (C3S) Climate Data Store (CDS)*. https://doi.org/10.24381/cds.bd0915c6

Hersbach, H., Bell, B., Berrisford, P., Biavati, G., Horányi, A., Muñoz Sabater, J., et al. (2023b). ERA5 hourly data on single levels from 1940 to present [Dataset]. *Copernicus Climate Change Service (C3S) Climate Data Store (CDS)*. https://doi.org/10.24381/cds.adbb2d47

Hersbach, H., Bell, B., Berrisford, P., Hirahara, S., Horányi, A., Muñoz-Sabater, J., et al. (2020). The ERA5 global reanalysis. *Quarterly Journal of the Royal Meteorological Society*, *146*(730), 1999–2049. https://doi.org/10.1002/qj.3803

Hersbach, H., Comyn-Platt, E., Bell, B., Berrisford, P., Biavati, G., Horányi, A., et al. (2023). ERA5 post-processed daily-statistics on pressure levels from 1940 to present [Dataset]. *Copernicus Climate Change Service (C3S) Climate Data Store (CDS)*. https://doi.org/10.24381/cds.4991cf48

Hitchcock, P., Polichtchouk, I., & Stockdale, T. (2024). Stratospheric Nudging And Predictable Surface Impacts (SNAPSI): Data produced by the IFS model at ECMWF [Dataset]. *NERC EDS Centre for Environmental Data Analysis*. http://catalogue.ceda.ac.uk/uuid/d160e81ccf9842d0b1c0a25b56a5ddfa/

Hitchcock, P. B., Butler, A., Charlton-Perez, A., Garfinkel, C. I., Stockdale, T., Anstey, J., et al. (2022). Stratospheric Nudging And Predictable Surface Impacts (SNAPSI): A protocol for investigating the role of stratospheric polar vortex disturbances in subseasonal to seasonal forecasts. *Geoscientific Model Development*, *15*(13), 5073–5092. https://doi.org/10.5194/gmd-15-5073-2022

Huang, W. T. K., Charlton-Perez, A., Lee, R. W., Neal, R., Sarran, C., & Sun, T. (2020). Weather regimes and patterns associated with temperature-related excess mortality in the UK: A pathway to sub-seasonal risk forecasting. *Environmental Research Letters*, *15*(12), 124052. https://doi.org/10.1088/1748-9326/abcbba

Kautz, L., Polichtchouk, I., Birner, T., Garny, H., & Pinto, J. G. (2020). Enhanced extended-range predictability of the 2018 late-winter Eurasian cold spell due to the stratosphere. *Quarterly Journal of the Royal Meteorological Society*, *146*(727), 1040–1055. https://doi.org/10.1002/qj.3724

Kim, H., & Hyun, Y.-K. (2024). Stratospheric Nudging And Predictable Surface Impacts (SNAPSI): Data produced by the GloSea6-GC32 model at KMA [Dataset]. *NERC EDS Centre for Environmental Data Analysis*. http://catalogue.ceda.ac.uk/uuid/81516f7545ef4ba1b39ec87ed5d0e5f1/

Knight, J. (2024). Stratospheric Nudging And Predictable Surface Impacts (SNAPSI): Data produced by the GloSea6 model at UKMO [Dataset]. *NERC EDS Centre for Environmental Data Analysis*. http://catalogue.ceda.ac.uk/uuid/8fc98ddf822f464dbd8a9e89b2da063c/

Knight, J., Scaife, A., Bett, P. E., Collier, T., Dunstone, N., Gordon, M., et al. (2021). Predictability of European winters 2017/2018 and 2018/2019: Contrasting influences from the tropics and stratosphere. *Atmospheric Science Letters*, *22*(1), e1009. https://doi.org/10.1002/asl.1009

Kretschmer, M., Cohen, J., Matthias, V., Runge, J., & Coumou, D. (2018). The different stratospheric influence on cold-extremes in Eurasia and North America. *Npj Climate and Atmospheric Science*, *1*(1), 44. https://doi.org/10.1038/s41612-018-0054-4

Kretschmer, M., Coumou, D., Agel, L., Barlow, M., Tziperman, E., & Cohen, J. (2018). More-persistent weak stratospheric polar vortex states linked to cold extremes. *Bulletin of the American Meteorological Society*, *99*(1), 49–60. https://doi.org/10.1175/bams-d-16-0259.1

Lee, R. W., Woolnough, S. J., Charlton-Perez, A. J., & Vitart, F. (2019). ENSO modulation of MJO teleconnections to the North Atlantic and Europe. *Geophysical Research Letters*, *46*(22), 13535–13545. https://doi.org/10.1029/2019gl084683

Lee, S. H., Charlton-Perez, A. J., Woolnough, S. J., & Furtado, J. C. (2022). How do stratospheric perturbations influence North American weather regime predictions? *Journal of Climate*, *35*(18), 5915–5932. https://doi.org/10.1175/jcli-d-21-0413.1

Lee, S. H., Furtado, J. C., & Charlton-Perez, A. J. (2019). Wintertime North American weather regimes and the Arctic stratospheric polar vortex. *Geophysical Research Letters*, *46*(24), 14892–14900. https://doi.org/10.1029/2019gl085592

Limpasuvan, V., Hartmann, D. L., Thompson, D. W. J., Jeev, K., & Yung, Y. L. (2005). Stratosphere-troposphere evolution during polar vortex intensification. *Journal of Geophysical Research*, *110*(D24), D24101. https://doi.org/10.1029/2005jd006302

Limpasuvan, V., Thompson, D. W. J., & Hartmann, D. L. (2004). The life cycle of the Northern Hemisphere sudden stratospheric warmings. *Journal of Climate*, *17*(13), 2584–2596. https://doi.org/10.1175/1520-0442(2004)017<2584:TLCOTN>2.0.CO;2

Lin, H., & Muncaster, R. (2024). Stratospheric Nudging And Predictable Surface Impacts (SNAPSI): Data produced by the GEM-NEMO model at ECCC [Dataset]. *NERC EDS Centre for Environmental Data Analysis*. http://catalogue.ceda.ac.uk/uuid/0760dcb81380402f8e7a1dcb20d1eec9/

Mariotti, A., Baggett, C., Barnes, E. A., Becker, E., Butler, A. H., Collins, D. C., et al. (2020). Windows of opportunity for skillful forecasts subseasonal to seasonal and beyond. *Bulletin of the American Meteorological Society*, *101*(5), E608–E625. https://doi.org/10.1175/bams-d-18-0326.1

Mastrangelo, D. (2024). Stratospheric Nudging And Predictable Surface Impacts (SNAPSI): Data produced by the GLOBO model at CNR-ISAC [Dataset]. *NERC EDS Centre for Environmental Data Analysis*. http://catalogue.ceda.ac.uk/uuid/181b2e501be0452984371d1c77fdab2a/

Maycock, A. C., Masukwedza, G. I. T., Hitchcock, P., & Simpson, I. R. (2020). A regime perspective on the North Atlantic eddy-driven jet response to sudden stratospheric warmings. *Journal of Climate*, *33*(9), 3901–3917. https://doi.org/10.1175/jcli-d-19-0702.1

Messori, G., & Dorrington, J. (2023). A joint perspective on North American and Euro-Atlantic weather regimes. *Geophysical Research Letters*, *50*(21), e2023GL104696. https://doi.org/10.1029/2023gl104696

Messori, G., Kretschmer, M., Lee, S. H., & Wendt, V. (2022). Stratospheric downward wave reflection events modulate North American weather regimes and cold spells. *Weather and Climate Dynamics*, *3*(4), 1215–1236. https://doi.org/10.5194/wcd-3-1215-2022

Michelangeli, P.-A., Vautard, R., & Legras, B. (1995). Weather regimes: Recurrence and quasi stationarity. *Journal of the Atmospheric Sciences*, *52*(8), 1237–1256. https://doi.org/10.1175/1520-0469(1995)052<1237:WRRAQS>2.0.CO;2

Millin, O. T., Furtado, J. C., & Basara, J. B. (2022). Characteristics, evolution, and formation of cold air outbreaks in the Great Plains of the United States. *Journal of Climate*, *35*(14), 4585–4602. https://doi.org/10.1175/jcli-d-21-0772.1

Pedregosa, F., Varoquaux, G., Gramfort, A., Michel, V., Thirion, B., Grisel, O., et al. (2011). Scikit-learn: Machine learning in python. *Journal of Machine Learning Research*, *12*(85), 2825–2830. Retrieved from http://jmlr.org/papers/v12/pedregosa11a.html

Robertson, A. W., Vigaud, N., Yuan, J., & Tippett, M. K. (2020). Toward identifying subseasonal forecasts of opportunity using North American weather regimes. *Monthly Weather Review*, *148*(5), 1861–1875. https://doi.org/10.1175/mwr-d-19-0285.1

Scaife, A. A., Karpechko, A. Y., Baldwin, M. P., Brookshaw, A., Butler, A. H., Eade, R., et al. (2015). Seasonal winter forecasts and the stratosphere. *Atmospheric Science Letters*, *17*(1), 51–56. https://doi.org/10.1002/asl.598

Schutte, M. K., Portal, A., Lee, S. H., & Messori, G. (2025). Dynamics of stratospheric wave reflection over the North Pacific. *Weather and Climate Dynamics*, *6*(2), 521–548. https://doi.org/10.5194/wcd-6-521-2025

Sigmond, M., Scinocca, J. F., Kharin, V. V., & Shepherd, T. G. (2013). Enhanced seasonal forecast skill following stratospheric sudden warmings. *Nature Geoscience*, *6*(2), 98–102. https://doi.org/10.1038/ngeo1698

Simpson, I., & Richter, J. (2024). Stratospheric Nudging And Predictable Surface Impacts (SNAPSI): Data produced by the CESM2-CAM6 model at NCAR [Dataset]. *NERC EDS Centre for Environmental Data Analysis*. http://catalogue.ceda.ac.uk/uuid/ce8fb52804934952a00ef7d3d223d305/

Son, S.-W., & Hong, D.-C. (2024). Stratospheric Nudging And Predictable Surface Impacts (SNAPSI): Data produced by the GRIMs model at SNU [Dataset]. *NERC EDS Centre for Environmental Data Analysis*. http://catalogue.ceda.ac.uk/uuid/8210180b4c664012831f8a66c934c004/

19448007, 2025, 15, Downloaded from https://agupubs.onlinelibrary.wiley.com/doi/10.1029/2025GL115668 by Test, Wiley Online Library on [07/08/2025]. See the Terms and Conditions (https://onlinelibrary.wiley.com/terms-and-conditions) on Wiley Online Library for rules of use; OA articles are governed by the applicable Creative Commons License

Specq, D. (2024). Stratospheric Nudging And Predictable Surface Impacts (SNAPSI): Data produced by the CNRM-CM 6.1 model at Météo France [Dataset]. *NERC EDS Centre for Environmental Data Analysis*. http://catalogue.ceda.ac.uk/uuid/201dac63fd1046e39299801dbf47dd3f/

Tripathi, O. P., Charlton-Perez, A., Sigmond, M., & Vitart, F. (2015). Enhanced long-range forecast skill in boreal winter following stratospheric strong vortex conditions. *Environmental Research Letters*, *10*(10), 104007. https://doi.org/10.1088/1748-9326/10/10/104007

van der Wiel, K., Bloomfield, H. C., Lee, R. W., Stoop, L. P., Blackport, R., Screen, J. A., & Selten, F. M. (2019). The influence of weather regimes on European renewable energy production and demand. *Environmental Research Letters*, *14*(9), 094010. https://doi.org/10.1088/1748-9326/ab38d3

White, C. J., Domeisen, D. I. V., Acharya, N., Adefisan, E. A., Anderson, M. L., Aura, S., et al. (2022). Advances in the application and utility of subseasonal-to-seasonal predictions. *Bulletin of the American Meteorological Society*, *103*(6), E1448–E1472. https://doi.org/10.1175/bams-d-20-0224.1

White, I., Garfinkel, C. I., Gerber, E. P., Jucker, M., Hitchcock, P., & Rao, J. (2020). The generic nature of the tropospheric response to sudden stratospheric warmings. *Journal of Climate*, *33*(13), 5589–5610. https://doi.org/10.1175/jcli-d-19-0697.1

19448007, 2025, 15, Downloaded from https://agupubs.onlinelibrary.wiley.com/doi/10.1029/2025GL115668 by Test, Wiley Online Library on [07/08/2025]. See the Terms and Conditions (https://onlinelibrary.wiley.com/terms-and-conditions) on Wiley Online Library for rules of use; OA articles are governed by the applicable Creative Commons License